Three-dimensional MREIT Simulator (MREITSim)

Atul S. Minhas, Zijun Meng, Young Tae Kim,
Hyung Joong Kim and Eung Je Woo
Department of Biomedical Engineering,
Kyung Hee University,
Gyeonggi-do, South Korea

Hyea Hyun Kim
Department of Applied Mathematics,
Kyung Hee University,
Gyeonggi-do, South Korea

***Abstract*—Magnetic resonance electrical impedance tomography (MREIT) is being developed to produce high-resolution cross-sectional conductivity images of an object. In MREIT, we scan the imaging object using an MRI scanner while injecting low-frequency current through surface electrodes. This produces change in the phase of precessing protons which is reflected in the MRI phase image. The conductivity imaging method in MREIT is thus based on static bioelectromagnetism and physics of MRI. In this paper, we describe a three-dimensional MREIT simulator (MREITSim) to numerically simulate the underlying physical phenomena in MREIT. We demonstrate the static bioelectromagnetism simulation and MREIT *k*-space data simulation as applications of this simulator. The simulator will be useful in developing new MREIT pulse sequences and conductivity image reconstruction algorithms.**

Keywords-MREIT, bioelectromagnetism, MRI, simulation

I. INTRODUCTION

In magnetic resonance electrical impedance tomography (MREIT) research, we need to quantitatively understand the static bioelectromagnetic phenomena inside the human body subject to an injected low-frequency current. This requires us to numerically solve a partial differential equation of the induced voltage u with a Neumann boundary condition [1]. Accurate calculations of voltage, current density and magnetic flux density are not trivial for a three-dimensional object with a general boundary shape and a presumed conductivity distribution. In order for the computational tool to be a complete MREIT simulator, we have to incorporate the computed magnetic flux density into an adopted MRI data collection process using a specific pulse sequence. This kind of integrated simulator incorporating both static bioelectromagnetism and MRI physics will enable us to produce *k*-space data sets for a given setting of an MREIT imaging experiment.

In this paper, we describe a developed three-dimensional MREIT simulator. Given an imaging object with a presumed conductivity distribution and electrode configuration, it generates a three-dimensional finite element model of the object to solve the partial differential equation of the induced voltage. Computing the current density distribution from the voltage and conductivity, it provides numerical tools to compute the induced magnetic flux density distribution. Incorporating the z-component of the induced magnetic flux density to MR phase images, the simulator synthesizes k-space MR data, which one would collect from the imaging object by using an MRI scanner. Including noise terms based upon the MREIT noise analysis, the simulator functions as a virtual MREIT scanner replacing expensive MREIT scans and provides quantitative numerical results of intended experimental studies.

We will demonstrate by showing examples that the simulator is very useful in understanding the related bioelectromagnetic phenomena and MR data collection process in MREIT. We will suggest the simulator as a basic research tool for future MREIT studies of its theory, algorithm and experimental technique. The simulator will be also useful to validate an experimental procedure.

II. THREE DIMENSIONAL MREIT SIMULATOR

A. Boundary value problem in MREIT

Let S denotes a three-dimensional electrically conducting object with its boundary ∂S as shown in Fig. 1(a). The four electrodes are denoted as E_1 to E_4 with their outer faces as F_1 to F_4. H_1 to H_4 denote the four electrode recession materials. We define the two regions of recessions and electrodes as $H = H_1 \cup H_2 \cup H_3 \cup H_4$ and $E = E_1 \cup E_2 \cup E_3 \cup E_4$, respectively. Fig. 1(b) shows the magnified view showing electrode E_1, its face F_1 and the recession material H_1. We let D be the region including the subject, recession materials and electrodes, that is, $D = S \cup H \cup E$ with its boundary ∂D. Current I is injected through the face F_1 of electrode E_1 and face F_3 of electrode E_3 which is connected to the ground. The induced voltage u in D satisfies the following boundary value problem with the Neumann and Dirichlet boundary conditions [2], [3]:

$$\begin{cases} \nabla \cdot (\sigma \nabla u) = 0 & \text{in } D \\ -\sigma \nabla u \cdot \mathbf{n} = 0 & \text{on } \partial D - F_1 - F_3 \\ -\sigma \nabla u \cdot \mathbf{n} = J_n & \text{on } F_1 \\ u = 0 & \text{on } F_3 \end{cases} \tag{1}$$

where **n** is the outward unit normal vector on ∂D, J_n is a normal component of the current density on face F_1 due to I and σ is the distribution of conductivity in D.

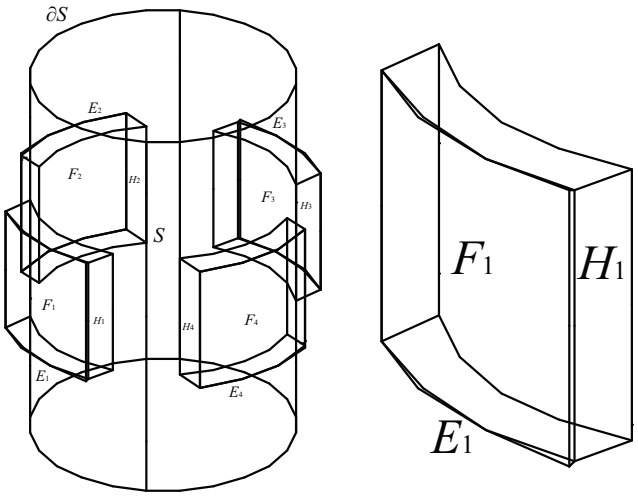

Figure 1. (a) Three-dimensional domain with recessed electrodes. (b) Magnified view showing electrode E_1, its face F_1 and recession material H_1.

B. Computation of voltage and current density using finite element model

We solve the boundary value problem in (1) using a finite element model of the object *S*. Such modeling can be done in a commercial software such as COMSOL (COMSOL Inc., USA), which provides an environment to numerically solve partial differential equations (PDEs) using the finite element method (FEM). It also supports programming through the MATLAB (The Mathworks Inc., USA) environment. We can implement the complete system of equations from (1) in COMSOL's AC-DC module by setting various parameters in the general electromagnetic PDE formulation available in the module for quasi-static problems. We set the boundary conditions and material properties for each sub-domain in the main domain and discretize the domain with an adaptive mesh. The matrix equation obtained after meshing can be solved using various linear and non-linear solvers available in the software package. From the solution u, the current density can be calculated as:

$$\mathbf{J} = -\sigma \nabla u \,. \tag{2}$$

The solution u and current density **J** can be interpolated over a regular grid with the `postinterp` command using a MATLAB based script program.

C. Numerical computation of magnetic flux density

We can compute the magnetic flux density from **J** in (2) as follows [2], [3]:

$$\mathbf{B}(\mathbf{r}) = \frac{\mu_0}{4\pi} \int \mathbf{J}(\mathbf{r}') \times \frac{\mathbf{r} - \mathbf{r}'}{|\mathbf{r} - \mathbf{r}'|^3} d\mathbf{r}' \,. \tag{3}$$

Considering $\mathbf{r} \in R^3$, this is a three-dimensional integral problem, with a time cost of $(N_x \times N_y)^2 \times N_z \times n_s$, where, N_x, N_y and N_z are the number of nodes in x, y, and z-direction and n_s is the number of planes where we calculate B_z. In order to compute B_z using (3), we developed a C code which uses **J** interpolated over a regular grid of $N_x \times N_y \times N_z$ using the COMSOL's post-processing function `postinterp`.

D. Simulation of MREIT B_z measurement

In MREIT, we synchronize the current injection pulse with the RF pulse in MRI to inject current in two different polarities [4]. The current injection adds an extra phase to the precessing protons which is reflected in the MRI k-space signal as follows:

$$S^{\pm}(m,n) = \iint M e^{j\delta} e^{\pm j\gamma B_z T_c} e^{-j(xm\Delta k_x + yn\Delta k_y)} dxdy \tag{4}$$

where γ is the gyromagnetic ratio, δ is the systematic phase artifact, T_c is the current injection duration, M is the MR magnitude signal, which may be a function of RF and main field-inhomogeneity, T_1, T_2, TR, TE, and flip angle [5]-[7]. Knowing various MRI scan parameters and assuming certain field-inhomogeneity distribution, we can simulate M, Δk_x and Δk_y. Using these quantities and the computed B_z obtained using the method described in section II-B, we can numerically compute the signal $S^{\pm}$ using (4). Taking the inverse Fourier transform of $S^{\pm}$ gives us the synthetic complex spatial domain signals $M^{\pm}$ with two different polarities for current injection as follows:

$$M^{\pm}(x,y) = M e^{j\delta} e^{\pm j\gamma B_z T_c} \,. \tag{5}$$

Taking the ratio of M^+ and M^- signals cancels out δ and provides the phase ψ due to B_z as follows:

$$e^{j\psi(x,y)} = e^{j2\gamma B_z T_c} = \frac{M^+(x,y)}{M^-(x,y)} \,. \tag{6}$$

From (6), we can calculate the phase ψ and magnetic flux density B_z as follows:

$$\begin{cases} \psi(x,y) = \arg\left(\dfrac{M^+(x,y)}{M^-(x,y)} \right) = 2\gamma B_z(x,y) T_c \\ B_z(x,y) = \dfrac{\psi(x,y)}{2\gamma T_c} \end{cases} \,. \tag{7}$$

The synthetic B_z measurement in (7) obtained from synthetic MRI k-space data must be equal to the numerical B_z obtained by method explained in section II-C, when no noise is assumed in data.

III. Numerical Example Model

A. Example model

We built a three-dimensional cylindrical phantom model using MATLAB based script program calling various functions unique to COMSOL's library. Using such functions, we could make a solid circle of diameter 100 mm and extrude it to make a cylinder of height 150 mm. This object is shown in Fig. 2(a). We made four recessions of 10 mm thickness and 50×50 mm^2 cross-sectional area as shown in Fig. 2(b).

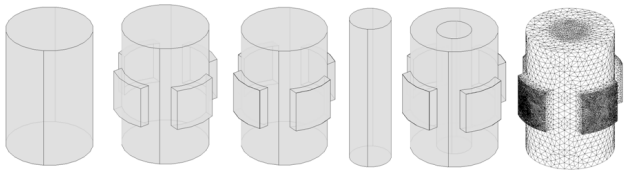

(a) (b) (c) (d) (e) (f)

Figure 2. (a) Model of a uniform cylindrical phantom. The same phantom with recession material attached to it is shown in (b) and with carbon electrodes attached is shown in (c). A solid cylindrical anomaly is shown in (d) and this anomaly added to model in (c) is shown in (e). The mesh for model in (e) is shown in (f).

Four carbon electrodes of 0.3 mm thickness were modeled around the recessions. Using the Boolean operators of addition and subtraction we could combine all these objects to make a composite model consisting of a uniform cylindrical background with electrodes and recession materials attached around it, as shown in Fig. 2(c). We made a solid cylindrical anomaly of 150 mm height and 40 mm diameter as shown in Fig. 2(d). We placed it at the center of the cylindrical background to make a phantom model shown in Fig. 2(e).

*B. Numerical computation of u, **J** and B_z*

The phantom model was meshed for numerical computations using an adaptive mesh shown in Fig. 2(f). It had 315,398 elements and 2,924,784 degrees of freedom. The conductivities of various objects in the model are shown in Table I. We solved (1) for u using the method explained in section II-B. We injected I=20 mA current through the outer face F_1 of electrode E_1. The boundary conditions used were $J_n=I/A$ over the face F_1 and u=0 over the face F_3. Here, A=0.002569 m^2 is the surface area of the electrode. The current density **J** was calculated using (2) and interpolated over a three-dimensional grid of size 128×128×200. We chose the x-y grid dimension in such a way that it matches with the field of view in a typical MREIT experiment. Using **J**, we computed B_z, the z-component of **B**, at the central plane of the model, using the method described in section II-C.

TABLE I. CONDUCTIVITIES OF VARIOUS OBJECTS IN PHANTOM MODEL.

Object	Electrode	Recession	Background	Anomaly
Conductivity [S/m]	24,000	1	1	10^{-50}

IV. RESULTS

Fig. 3(a)-(c) shows the voltage distribution u, total current density J, and z-component of magnetic flux density B_z, along the central plane of the model for current injection between F_1 and F_3. The high current density due to edge effect can be seen in the current density image (b) underneath the current carrying electrodes near recession. A similar observation can be made from image (c) where there is high magnetic flux density near the edges.

Fig. 4 shows the simulation results of MREIT B_z measurement as explained in section II-D. The values of various parameters assumed to simulate (4) were T_c=17 ms and δ=0. The k-space data was simulated by adding a random noise of normal distribution N(0,0.001) to the magnitude image M. The images in (a) and (b) are the real and imaginary parts of the k-space image S^+. The images in (c) and (d) are the magnitude and phase parts of the complex spatial-domain MR image M^+. The images from (f) to (i) are the corresponding images for negative current injection. The original noise free B_z image used to synthesize the k-space signal in (4) is shown in (e). The image in (j) shows the synthetic B_z measurement obtained using (7).

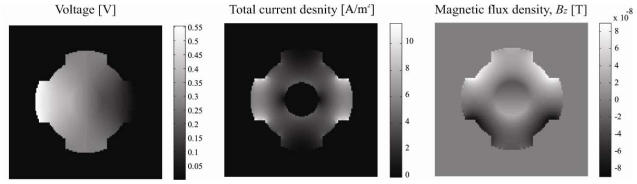

(a) (b) (c)

Figure 3. Simulation results for the cylindrical phantom model with a solid cylindrical insulating anomaly at its center. The image in (a) is voltage, (b) shows the absolute current density, and (c) shows the magnetic flux density for current injection between F_1 and F_3.

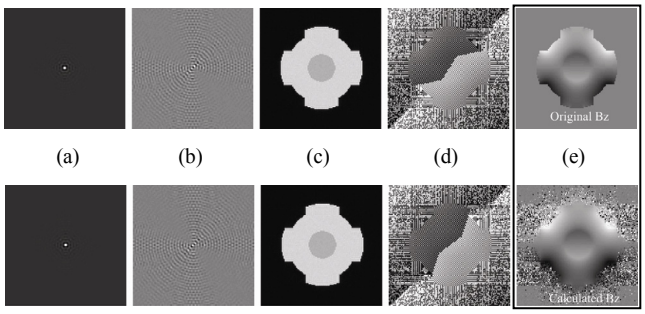

(a) (b) (c) (d) (e)

(f) (g) (h) (i) (j)

Figure 4. Simulation of MREIT B_z measurement using the cylindrical phantom model with a solid cylindrical insulating anomaly at its center. The images in (a) and (b) are the real and imaginary parts respectively, of the k-space image S^+, (c) and (d) are the magnitude and phase parts of the complex spatial-domain MR image M^+. The images from (f) to (i) are the corresponding images for negative current injection. The image in (e) is the original B_z image used to simulate the k-space image S^+. The image in (j) is the synthetic B_z measurement obtained using (7).

It can be observed in (j) that there are pixels with wrapped phase of ±π around the phantom boundary. This wrapped phase is much higher along the current injection direction than along the non-current injection direction. We can have similar observation from the MREIT experimental data reported in other studies [6], [7]. The results in Fig. 4 demonstrate the capability of MREIT simulator to synthesize the MREIT k-space data and B_z measurement process successfully.

V. DISCUSSION AND CONCLUSION

We described a COMSOL based three-dimensional MREIT simulator. The simulator was capable of making three-dimensional phantom geometries and generates their finite element models. It could compute the current injection induced bioelectromagnetic quantities viz. voltage, current density and magnetic flux density. Utilizing the z-component

of magnetic flux density, the simulator could synthesize the MREIT *k*-space data. The synthetic B_z measurement showed wrapped phase around the phantom boundary which matches with the observations made from experimental data.

The proposed simulator is based on the software package COMSOL. Using this software provided us the liberty of performing the complete cycle of simulations from geometry modeling to post-processing of numerical solution in same environment. Using the library of MATLAB functions provided by the package, we could take the advantage of MATLAB script programming for model making and numerical computations. The adaptive meshing feature in the package allowed meshing of geometry model efficiently. We could also subjectively modify the meshes of various sub-domains to further enhance the numerical accuracy and increase the convergence speed of solution.

Considering the spin echo pulse sequence for simulation of MREIT B_z measurement, we could assume the magnitude image independent of the main field inhomogeneity, T_1, T_2, *TR*, *TE*, and flip angle. However, if we consider gradient echo based pulse sequences [8] and other fast pulse sequences [5], then the signal would be dependent on those parameters. The MREIT simulator described here can be extended directly to those MRI simulations.

The accuracy of the proposed simulator is affected by geometry modeling, meshing of different sub-domains, and the size of the regular grid chosen for interpolation. Increasing the size of grid would increase the accuracy of B_z at the cost of increase in computation time. This time would further increase with the increase in the number of planes n_s chosen for B_z calculation. This issue can be addressed by using faster methods of B_z computation like Poisson's solver suggested in other studies [2]. We would implement this solver in our future versions of MREITSim.

Using this simulator, we can obviate certain MREIT algorithm and pulse sequence validation experiments. It could be helpful in designing the MREIT experiments optimally. We may study the effect of location and shape of electrodes on the bioelectromagnetic quantities in MREIT. We can also analyze those simulated quantities to understand the current flow in various parts of human body including leg, knee and brain. This would help us in interpreting the *in-vivo* human tissue conductivity images reconstructed using harmonic B_z algorithm in MREIT [9]. Novel designs of stable phantoms in MREIT could also be proposed based on simulations.

In further developments, we would modify the simulator to include the modeling of current carrying wires. Following this, we will validate our simulator by comparing the computed B_z with the analytical and experimentally measured B_z. We also plan to study the effect of anisotropic conductivity in future versions. We would further enhance our simulator by including the effects of the fluctuations of magnetic field of main magnet, RF magnetic fields and gradient fields on the *k*-space data acquisition and B_z computations. The bioelectromagnetism of B1 mapping [10] would also be included to study the MREIT and MREPT [11] physics using this simulator.

ACKNOWLEDGMENT

This work was supported by the National Research Foundation of Korea (NRF) grant funded by the Korea government (MEST) (No. 20100018275).

REFERENCES

[1] E. J. Woo, J. K. Seo, and S. Y. Lee, Magnetic resonance electrical impedance tomography (MREIT) in Holder D ed., Electrical Impedance Tomography: Methods, History and Applications, Bristol, UK: IOP Publishing, pp. 239-291, 2005.

[2] B. I. Lee, S. H. Oh, E. J. Woo, S. Y. Lee, M. H. Cho, O. Kwon, J. K. Seo, J. Y. Lee, and W. S. Baek, "Three-dimensional forward solver and its performance analysis in magnetic resonance electrical impedance tomography (MREIT) using recessed electrodes," Phys. Med. Biol., vol. 48, pp. 1971-1986, 2003.

[3] Y. Z. Ider, and O. Birgul, "Use of the magnetic field generated by the internal distribution of injected currents for electrical impedance tomography (MR-EIT)," Elektrik, vol. 6, pp. 215-225, 1998.

[4] C. Park, B. I. Lee, O. Kwon, and E. J. Woo, "Measurement of induced magnetic flux density using injection current nonlinear encoding (ICNE) in MREIT," Physiol. Meas., vol. 28, pp. 117-127, 2006.

[5] A. S. Minhas, E. J. Woo, and S. Y. Lee, "Magnetic flux density measurement with balanced steady-state free precession pulse sequence for MREIT: a simulation study," in Proc. IEEE EMBC 2009, Minneapolis, Minnesota, USA, pp. 2276-2278, 2009.

[6] S. H. Oh, B. I. Lee, T. S. Park, S. Y. Lee, E. J. Woo, M. H. Cho, O. Kwon, and J. K. Seo, "Magnetic resonance electrical impedance tomography at 3 Tesla field strength," Mag. Reson. Med., vol. 51, pp. 1292-1296, 2004.

[7] E. J. Woo and J. K. Seo, "Magnetic resonance electrical impedance tomography (MREIT) for high-resolution conductivity imaging," Physiol. Meas., vol. 29, pp. R1-R26, 2008.

[8] M. A. Bernstein, K. F. King, and X. J. Zhou, Handbook of MRI pulse sequences, London, UK: Elsevier Academic Press, 2004.

[9] K. Jeon, C-O Lee, H. J. Kim, E. J. Woo, and J. K. Seo, "CoReHA: conductivity reconstructor using harmonic algorithms for magnetic resonance electrical impedance tomography (MREIT)," J. Biomed. Eng. Res., vol. 30, pp. 279-287, 2009.

[10] R. Stollberger, and P. Wach, "Imaging the active B_1 field in vivo," Mag. Reson. Med., vol. 35, pp. 246-251, 1996.

[11] U. Katscher, T. Viogt, C. Findeklee, P. Vernickel, K. Nehrke, and O. Dossel, "Determination of electric conductivity and local SAR via B1 mapping," IEEE Trans. Med. Imag., vol. 28, pp. 1365-1374, 2009.